# A Simple 24-Pulse Rectifier Employing an Auxiliary Pulse-Doubling Circuit

Jingfang Wang, *Member, IEEE*, Anchen Chen, Xuliang Yao, Lei Li, Yusheng Lv, and Qiming Chen, *Member, IEEE*

***Abstract*—A simple 24-pulse rectifier that provides low-harmonic utility power interface is proposed in this article. The proposed 24-pulse rectifier consists of a 12-pulse rectifier using a zigzag phase-shifting transformer and an auxiliary pulse-doubling circuit (APDC). Two auxiliary diodes in the APDC extract specific rectangular currents from the dc side of the rectifier to modulate and increase the output states of three-phase rectification bridges first, and then the 12-pulse rectifier is extended to a 24-pulse rectifier in accordance with the current relationship between ac and dc sides. The main low-order harmonics, such as 11th and 13th, are reduced markedly from the input line current and the proposed rectifier draws near-sinusoidal input line currents with less than 5% THD from the utility. The maximum current flowing through the two auxiliary diodes in APDC is only 3.4% of the load current and the capacity of APDC is only 3.06% of the output power. Thus, the proposed scheme is inexpensive and easy to implement and has a simple circuit configuration. Theoretical analyses were experimentally verified using a 1.7-kW experimental prototype.**

***Index Terms*—Harmonics, multipulse rectifier, power quality, pulse doubling.**

## I. Introduction

THE 12-pulse rectifier has the advantages of simple circuit structure, high reliability, low cost, and low electromagnetic interference. It is often used as the interface between electrical equipment and power grid in high-power occasions, such as ship electric propulsion, urban rail power supply, metal smelting, and power supply to aircraft systems. However, when the 12-pulse rectifier is employed alone, it produces a large number of harmonics, which bring harmonic pollution to the power grid and affect the normal operation of other electrical equipment [1], [2].

Various harmonic suppression schemes are proposed to effectively reduce the current harmonics generated by the 12-pulse rectifier. They mainly include two kinds: one is to install passive and active filters on the ac side of the 12-pulse rectifier to compensate harmonics [3]–[5]. The passive filter has the advantages of simple structure, easy implementation, and low cost. However, its harmonic compensation ability is limited and it could only compensate for some characteristic harmonics. The harmonic suppression performance of an active power filter is good but the control is complex and the cost is high. The other one is to transform the structure of the 12-pulse rectifier for it to produce less or no harmonics [6]–[20]. In [11], the output current of the 12-pulse rectifier is modulated by a series of switch devices directly behind the rectifier bridge and the harmonics of the input current are significantly suppressed. However, two switching devices are directly connected in series in the load path, resulting in large current stress and switching loss. In [12]–[14], the active inter-phase reactor (AIPR) scheme was proposed to lower the input current harmonics of the 12-pulse rectifier. The input line current harmonics is effectively reduced by the injected triangle current generated by an AIPR. This method has a good harmonic suppression effect but the control of AIPR is relatively complex and it does not improve the output voltage. Increasing the pulse number of the rectifier is one of the most effective methods to suppress the input current harmonics and output voltage ripple at the same time. In [15]–[17], several 18-, 20-, and 24-pulse rectifiers were given by further increasing the output voltage phase number of the phase-shifting transformer. Compared with the 12-pulse rectifier, the above-mentioned rectifiers showed effectively decreased output voltage ripple and THD of the input line current. However, the structure of the phase-shifting transformer becomes more complex and the number of components is doubled, which increases the complexity and cost of the rectifier. A 24-pulse rectifier based on a double-tap changer was proposed to multiply the pulse number of the rectifier without increasing its complexity. It multiplies the pulse number of the rectifier from 12 to 24. This method has the advantages of simple circuit structure, high reliability, and easy implementation; however, the additional diodes on the tap are connected in series with the load and the total currents through two additional auxiliary diodes are 100% load currents. The current stress and conduction losses of the two additional auxiliary diodes are high [18]–[20]. A series-connected 24-pulse rectifier based on dc-side voltage injection is presented in [21] to effectively reduce the current stress and additional conduction loss of the auxiliary diodes in the tap changer. It modulates the output voltage state of the rectifier bridge by injecting square-wave voltage into the dc side

Manuscript received July 17, 2021; revised November 7, 2021; accepted December 31, 2021. Date of publication January 10, 2022; date of current version March 24, 2022. Recommended for publication by Associate Editor J. Liu. *(Corresponding author: Xuliang Yao.)*

Jingfang Wang, Xuliang Yao, Lei Li, and Yusheng Lv are with the College of Intelligent Systems Science and Engineering, Harbin Engineering University, Harbin 150001, China (e-mail: jingfangwang@hrbeu.edu.cn; yxlhrbeu2124@126.com; llhrbeu040015@126.com; 445610615@qq.com).

Anchen Chen is with CRRC Qingdao Sifang Rolling Stock Research Institute Co., Ltd., Qingdao 266031, China (e-mail: 363485154@qq.com).

Qiming Chen is with the School of Electrical Engineering and Automation, Harbin Institute of Technology, Harbin 150001, China (e-mail: chenqiming@hit.edu.cn).

Color versions of one or more figures in this article are available at https://doi.org/10.1109/TPEL.2022.3141705.

Digital Object Identifier 10.1109/TPEL.2022.3141705

of the rectifier. Then, in accordance with the voltage relationship between the ac and dc sides of the rectifier, the number of steps of the input voltage is increased to 24 steps, which contributes to the reduction for the harmonics of the input line current. This method has the advantages of simple circuit structure, low current stress of the auxiliary diode, and high reliability, but it belongs to the method of doubling the number of input voltage steps of the rectifier. It must connect three sufficiently large inductors in series on the input side, which will not only increase the volume of the rectifier, weight, and cost, but also reduce the displacement factor (DF) of the rectifier, and make the output characteristics of the rectifier very soft. When the load current changes, the output voltage cannot be stabilized at a constant value. In [22], a 24-pulse 4-star rectifier with an auxiliary single-phase full-wave rectifier (ASFWR) on the dc side is proposed. It modulates and increases the output current states of the rectifier through the alternate conduction of auxiliary diodes in the ASFWR. The number of steps of the input current of the rectifier is increased to 24 according to the relationship between the ac- and dc-side currents, which effectively suppresses the harmonics of the input line current. The current flowing through the auxiliary diode is only 3.4% of the load current because the ASFWR is connected in parallel with the load. The current stress and the additional conduction loss generated by the auxiliary diodes are effectively reduced. However, more magnetic devices (two phase-shifting transformers, two conventional interphase reactors (IPRs), and a special IPR) are required, and the special IPR needs center-tapped secondary windings, which increase the cost and complexity of the rectifier. In [23], a 36-pulse ac–dc converter with a tapped interphase bridge rectifier on the dc side is proposed. The auxiliary diodes in the tapped interphase bridge rectifier alternately conduct, modulate, and increase the level of the output current of the rectifier. Then, on the basis of the relationship of ac- and dc-side currents, the number of steps of the input current of the rectifier is increased to 36 steps, further suppressing the input current harmonics. However, the tapped interphase bridge rectifier has a complicated structure; it requires the addition of a secondary winding with a center tap. Two auxiliary diodes in the tapped interphase bridge rectifier are connected in series in the load path; thus, they bear high-current stress and produce large additional conduction loss.

To effectively reduce the input line current THD and the current stress of the auxiliary diodes and further simplify the structure of the pulse multiplication circuit, this article proposes a 24-pulse rectifier with a new auxiliary pulse-doubling circuit (APDC). The proposed scheme has the following advantages.

1) The proposed 24-pulse rectifier is robust and simple to implement owing to its passive nature and few components.
2) Only a low capacity (3.06% $P_{\mathrm{d}}$) APDC is sufficient to extend the conventional 12-pulse rectifier to a simple 24-pulse rectifier. Thus, the proposed scheme is a cost-effective and highly efficient solution to harmonic pollution.
3) Compared with the double-tap changer scheme, the current stress of the additional auxiliary diodes is effectively reduced (from $I_{\mathrm{d}}$ to 3.4% $I_{\mathrm{d}}$) as the two auxiliary diodes in APDC are in parallel with the load, hence the lower additional conduction loss.

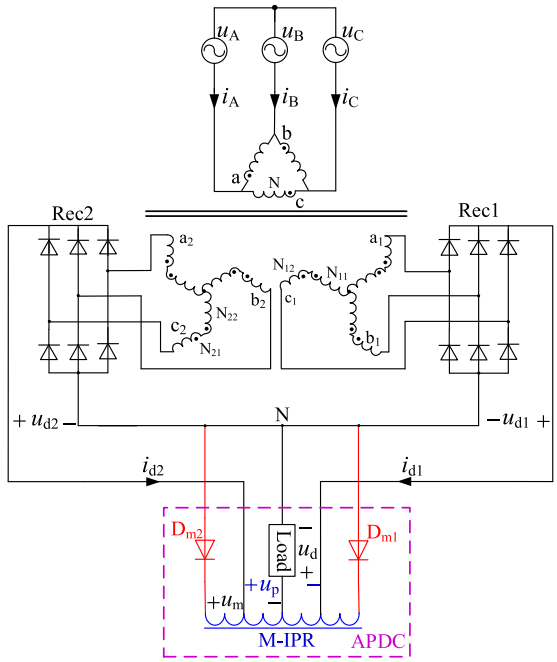


Fig. 1. Proposed 24-pulse rectifier with APDC at dc side.

4) When one of the auxiliary diodes in APDC has an open-circuit fault, the proposed APDC scheme still has a certain harmonic suppression capability and the proposed rectifier works as a quasi-18 pulse rectifier.

## II. Circuit Topology and Its Working Principle

### A. Proposed 24-Pulse Rectifier With APDC

Fig. 1 shows the proposed 24-pulse rectifier with APDC at the dc side.

As shown in Fig. 1, in addition to the APDC, the other parts of the proposed 24-pulse rectifier have a uniform structure, with the 12-pulse rectifier using a zigzag phase-shifting transformer. The APDC is made up of a modified IPR (M-IPR) and two auxiliary diodes ($\mathrm{D_{m1}}$ and $\mathrm{D_{m2}}$). Diodes $\mathrm{D_{m1}}$ and $\mathrm{D_{m2}}$ are connected in parallel with the load. This special connection aims to significantly reduce the current stress and additional conduction losses of $\mathrm{D_{m1}}$ and $\mathrm{D_{m2}}$. In addition, $\mathrm{D_{m1}}$ and $\mathrm{D_{m2}}$ in APDC conduct alternately and extract two specific rectangular currents from the dc side to modulate and increase the output currents and voltages state of the three-phase rectification bridges Rec1 and Rec2. Then, the 12-pulse rectifier is extended to a new 24-pulse rectifier in accordance with the current relationship between ac and dc sides and the voltage relationship on the dc side.

In Fig. 1, to realize 30° phase shifting, the turn ratio of the primary and secondary windings of the zigzag phase-shifting transformer meets

$$N : N_{11} : N_{12} : N_{21} : N_{22} = \sqrt{3} : k : \frac{\sqrt{3}-1}{2}k : k : \frac{\sqrt{3}-1}{2}k. \quad (1)$$

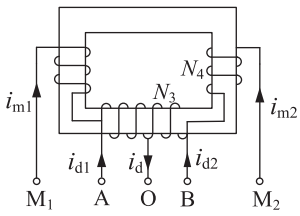


Fig. 2. Winding structure of M-IPR in APDC.

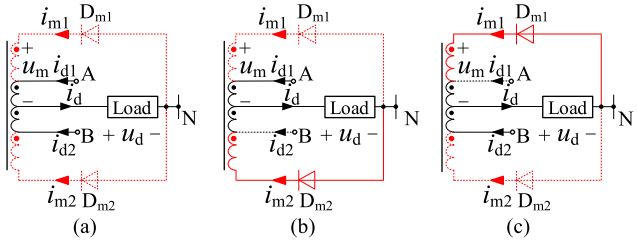


Fig. 3. Working modes of the proposed rectifier. (a) O mode. (b) N mode. (c) P mode.

Fig. 2 shows the winding structure of M-IPR in APDC.

For the convenience of later analysis, the tap position turn ratio $m$ of M-IPR in Fig. 2 is defined as

$$m = \frac{N_{\mathrm{M1O}}}{N_{\mathrm{AB}}} = \frac{N_{\mathrm{OM2}}}{N_{\mathrm{AB}}} = \frac{u_{\mathrm{m}}}{u_{\mathrm{p}}}. \tag{2}$$

### B. Operating Modes of the Proposed 24-Pulse Rectifier

In Fig. 1, in accordance with the relationship between the winding voltage $u_{\mathrm{m}}$ of M-IPR in APDC and load voltage $u_{\mathrm{d}}$, the proposed 24-pulse rectifier has three working modes: O mode, N mode, and P mode. The circuit diagram under the different modes is shown in Fig. 3.

*O Mode:* When $|u_{\mathrm{m}}|<u_{\mathrm{d}}$, APDC works in O mode [see Fig. 3(a)]. In this mode, the auxiliary diodes $\mathrm{D_{m1}}$ and $\mathrm{D_{m2}}$ in APDC are reverse-biased and OFF, and the currents flowing through $\mathrm{D_{m1}}$ and $\mathrm{D_{m2}}$ are $i_{\mathrm{m1}} = i_{\mathrm{m2}} = 0$. At this time, the proposed rectifier works as the conventional 12-pulse rectifier. The load in Fig. 1 is a large inductive load, and the load current $i_{\mathrm{d}}$ can be considered as a constant value $I_{\mathrm{d}}$.

According to Kirchhoff's current law (KCL) and magnetomotive force (MMF) equations of APDC, the relationship between output currents $i_{\mathrm{d1}}$ and $i_{\mathrm{d2}}$ of Rec1 and Rec2 and load current $i_{\mathrm{d}}$ is obtained as

$$i_{\mathrm{d1}} = i_{\mathrm{d2}} = \frac{1}{2} i_{\mathrm{d}} = \frac{1}{2} I_{\mathrm{d}}. \tag{3}$$

According to Kirchhoff's voltage law (KVL), the relationship between output voltage $u_{\mathrm{d1}}$ and $u_{\mathrm{d2}}$ of Rec1 and Rec2 and load voltage $u_{\mathrm{d}}$ is

$$u_{\mathrm{d}} = \frac{u_{\mathrm{d1}} + u_{\mathrm{d2}}}{2}. \tag{4}$$

*N Mode:* When $u_{\mathrm{m}} > u_{\mathrm{d}}$, the APDC operates in N mode [see Fig. 3(b)]. In this case, the auxiliary diode $\mathrm{D_{m1}}$ in APDC is reverse-biased and switched OFF, whereas the auxiliary diode $\mathrm{D_{m2}}$ is switched ON and its current $i_{\mathrm{m2}} > 0$. Rec1 is turned ON and its output current $i_{\mathrm{d1}} > 0$. Meanwhile, Rec2 is turned OFF, and its output current $i_{\mathrm{d2}} = 0$. In terms of KCL and the MMF equations of APDC, the relationship amongst current $i_{\mathrm{d}}$, $i_{\mathrm{m2}}$, and $i_{\mathrm{d}}$ is obtained as

$$\begin{cases} i_{\mathrm{d1}} \cdot \frac{N_{\mathrm{AB}}}{2} = i_{\mathrm{m2}} \cdot N_{\mathrm{OM2}} \\ i_{\mathrm{d1}} + i_{\mathrm{m2}} = i_{\mathrm{d}} = I_{\mathrm{d}}. \end{cases} \tag{5}$$

Substituting (2) into (5), $i_{\mathrm{d1}}$ and $i_{\mathrm{m2}}$ are obtained as

$$\begin{cases} i_{\mathrm{d1}} = \frac{2m}{2m+1} I_{\mathrm{d}} \\ i_{\mathrm{m2}} = \frac{1}{2m+1} I_{\mathrm{d}}. \end{cases} \tag{6}$$

According to KVL, the relationship between voltage $u_{\mathrm{d}}$, $u_{\mathrm{d1}}$, and $u_{\mathrm{d2}}$ is

$$\begin{cases} u_{\mathrm{d1}} - \frac{N_{\mathrm{AB}}}{2N_{\mathrm{M1O}}} u_{\mathrm{d}} = u_{\mathrm{d}} \\ u_{\mathrm{d1}} - \frac{N_{\mathrm{AB}}}{N_{\mathrm{M1O}}} u_{\mathrm{d}} = u_{\mathrm{d2}}. \end{cases} \tag{7}$$

Substituting (2) into (7), the voltages $u_{\mathrm{d}}$ and $u_{\mathrm{d2}}$ are

$$\begin{cases} u_{\mathrm{d}} = \frac{2m}{2m+1} u_{\mathrm{d1}} \\ u_{\mathrm{d2}} = \frac{2m-1}{2m+1} u_{\mathrm{d1}}. \end{cases} \tag{8}$$

*P Mode:* When $-u_{\mathrm{m}} > u_{\mathrm{d}}$, the APDC operates in P mode [see Fig. 3(c)]. At this point, the auxiliary diode $\mathrm{D_{m2}}$ in ADPC is reverse-biased and switched OFF, whereas the auxiliary diode $\mathrm{D_{m1}}$ is switched ON and its current $i_{\mathrm{m1}} > 0$. Rec2 is turned ON and its output current $i_{\mathrm{d2}} > 0$. Meanwhile, Rec1 is turned OFF and its output current $i_{\mathrm{d1}} = 0$. In accordance with KCL and the MMF equations of APDC, the relationship amongst current $i_{\mathrm{d2}}$, $i_{\mathrm{m1}}$, and $i_{\mathrm{d}}$ is

$$\begin{cases} i_{\mathrm{d2}} \cdot \frac{N_{\mathrm{AB}}}{2} = i_{\mathrm{m1}} \cdot N_{\mathrm{M1O}} \\ i_{\mathrm{d2}} + i_{\mathrm{m1}} = i_{\mathrm{d}} = I_{\mathrm{d}}. \end{cases} \tag{9}$$

Substituting (2) into (9), the currents $i_{\mathrm{m1}}$ and $i_{\mathrm{d2}}$ are obtained as

$$\begin{cases} i_{\mathrm{d2}} = \frac{2m}{2m+1} I_{\mathrm{d}} \\ i_{\mathrm{m1}} = \frac{1}{2m+1} I_{\mathrm{d}}. \end{cases} \tag{10}$$

According to KVL, the following relationship between the voltages $u_{\mathrm{d}}$, $u_{\mathrm{d1}}$, and $u_{\mathrm{d2}}$ is:

$$\begin{cases} u_{\mathrm{d2}} - \frac{N_{\mathrm{AB}}}{2N_{\mathrm{OM2}}} u_{\mathrm{d}} = u_{\mathrm{d}} \\ u_{\mathrm{d2}} - \frac{N_{\mathrm{AB}}}{N_{\mathrm{OM2}}} u_{\mathrm{d}} = u_{\mathrm{d1}}. \end{cases} \tag{11}$$

Substituting (2) into (11), the voltages $u_{\mathrm{d}}$ and $u_{\mathrm{d1}}$ are obtained as

$$\begin{cases} u_{\mathrm{d}} = \frac{2m}{2m+1} u_{\mathrm{d2}} \\ u_{\mathrm{d1}} = \frac{2m-1}{2m+1} u_{\mathrm{d2}}. \end{cases} \tag{12}$$

The above analysis shows that in accordance with the relationship between winding voltage $u_{\mathrm{m}}$ and load voltage $u_{\mathrm{d}}$, the APDC operates in different modes. The output current and voltage modes of Rec1 and Rec2 are added first, and then the pulse number of the rectifier is doubled. Fig. 4 shows the essential waveforms (under optimal turn ratio) of the proposed rectifier.

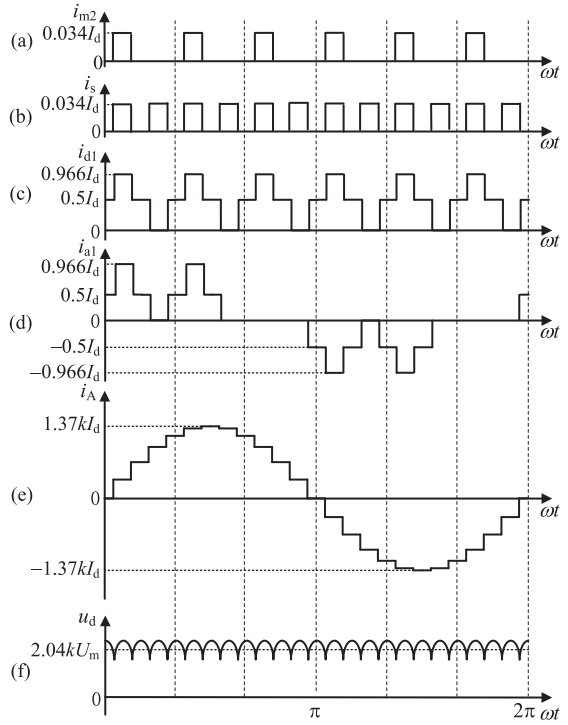


Fig. 4. Essential waveforms of the proposed rectifier. (a) Current $i_{\mathrm{m2}}$ flowing through $\mathrm{D_{m2}}$. (b) Rectangular current $i_{\mathrm{s}}$ ($i_{\mathrm{s}} = i_{\mathrm{m1}} + i_{\mathrm{m2}}$) extracted by APDC from the dc side. (c) Output current $i_{\mathrm{d1}}$ of Rec1. (d) Input current $i_{\mathrm{a1}}$ of Rec1. (e) Input current $i_{\mathrm{A}}$ of the proposed 24-pulse rectifier. (f) Output voltage $u_{\mathrm{d}}$ of the proposed 24-pulse rectifier.

## III. Critical and Optimal Turn Ratio of M-IPR in APDC

### A. Critical Turn Ratio of M-IPR in APDC

From Fig. 1 and the working modes of the rectifier, if the maximum value of the winding voltage $|u_{\mathrm{m}}|$ of the M-IPR is less than the minimum value of the load voltage $u_{\mathrm{d}}$, the auxiliary diodes $\mathrm{D_{m1}}$ and $\mathrm{D_{m2}}$ in APDC are reverse-biased. The proposed rectifier operates as a conventional 12-pulse rectifier. Therefore, to guarantee that APDC works normally, the maximum value of the winding voltage $|u_{\mathrm{m}}|$ of the M-IPR must be greater than the minimum value of the load voltage $u_{\mathrm{d}}$. Since the winding voltage $|u_{\mathrm{m}}|$ is determined by the turn ratio of M-IPR, the turn ratio that makes the auxiliary diodes $\mathrm{D_{m1}}$ and $\mathrm{D_{m2}}$ in APDC can conduction is the critical turn ratio of M-IPR. The critical turn ratio of M-IPR is analyzed as follows.

When the diodes $\mathrm{D_{m1}}$ and $\mathrm{D_{m2}}$ in APDC are not conducting, the proposed rectifier works as a 12-pulse rectifier. Set the input voltage of the rectifier as

$$\begin{cases} u_{\mathrm{A}} = U_{\mathrm{m}} \sin(\omega t) \\ u_{\mathrm{B}} = U_{\mathrm{m}} \sin(\omega t - 2\pi/3) \\ u_{\mathrm{C}} = U_{\mathrm{m}} \sin(\omega t + 2\pi/3) \end{cases} \tag{13}$$

where $U_{\mathrm{m}}$ is the amplitude of the input phase voltage of the rectifier.

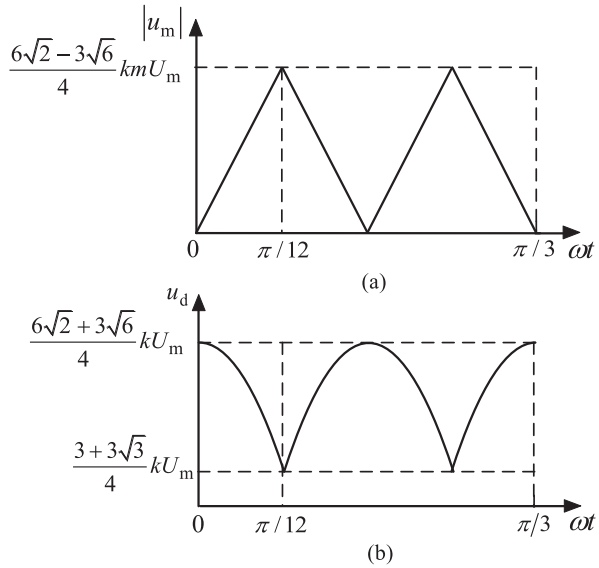


Fig. 5. Waveform of winding voltage $|u_{\mathrm{m}}|$ and load voltage $u_{\mathrm{d}}$. (a) Winding voltage $|u_{\mathrm{m}}|$. (b) Load voltage $u_{\mathrm{d}}$.

According to the rectifier structure shown in Fig. 1, the load voltage $u_{\mathrm{d}}$ can be obtained as

$$u_{\mathrm{d}} = \begin{cases} Y_1 kU_{\mathrm{m}} \cos(\omega t - \frac{h\pi}{3}) & \omega t \in [\frac{h\pi}{3}, \frac{h\pi}{3} + \frac{\pi}{12}] \\ Y_1 kU_{\mathrm{m}} \cos(\omega t - \frac{\pi}{6} - \frac{h\pi}{3}) & \omega t \in [\frac{h\pi}{3} + \frac{\pi}{12}, \frac{h\pi}{3} + \frac{\pi}{4}] \\ Y_1 kU_{\mathrm{m}} \cos(\omega t - \frac{\pi}{3} - \frac{h\pi}{3}) & \omega t \in [\frac{h\pi}{3} + \frac{\pi}{4}, \frac{h\pi}{3} + \frac{\pi}{3}] \end{cases} \tag{14}$$

where $Y_1 = \frac{3}{4}(1+\sqrt{3})$ and $h = 0,1,2,3,\ldots$

The winding voltage $u_m$ of M-IPR is

$$u_{\mathrm{m}} = \begin{cases} mkY_2 U_{\mathrm{m}} \sin(\omega t - \frac{h\pi}{3}) & \omega t \in [\frac{h\pi}{3}, \frac{h\pi}{3} + \frac{\pi}{12}] \\ mkY_2 U_{\mathrm{m}} \sin(\omega t - \frac{\pi}{6} - \frac{h\pi}{3}) & \omega t \in [\frac{h\pi}{3} + \frac{\pi}{12}, \frac{h\pi}{3} + \frac{\pi}{4}] \\ mkY_2 U_{\mathrm{m}} \sin(\omega t - \frac{\pi}{3} - \frac{h\pi}{3}) & \omega t \in [\frac{h\pi}{3} + \frac{\pi}{4}, \frac{h\pi}{3} + \frac{\pi}{3}] \end{cases} \tag{15}$$

where $Y_2 = \frac{3}{2}(\sqrt{3}-1)$ and $h = 0,1,2,3,\ldots$

According to (14) and (15), the waveforms of the load voltage $u_{\mathrm{d}}$ and the winding voltage $|u_{\mathrm{m}}|$ of M-IPR can be obtained as shown in Fig. 5(a) and (b). When $\omega t = \pi/12$, $u_{\mathrm{d}}$ gets the minimum value and $|u_{\mathrm{m}}|$ reaches the maximum value.

The M-IPR turns ratio that makes the diodes $\mathrm{D_{m1}}$ and $\mathrm{D_{m2}}$ in APDC conduct on satisfies

$$u_{\mathrm{d}}\big|_{\omega t = \frac{\pi}{12}} < m\,|u_{\mathrm{p}}|\big|_{\omega t = \frac{\pi}{12}}\,. \tag{16}$$

Substitute (14) and (15) into (16), we get

$$m > \frac{7+4\sqrt{3}}{2} = 6.964. \tag{17}$$

From (17), the critical turns ratio $m$ of M-IPR that enables diodes $\mathrm{D_{m1}}$ and $\mathrm{D_{m2}}$ in APDC conduct on is 6.964. It indicates that when the M-IPR turns ratio $m$ is less than or equal to 6.964, the rectifier works as a 12-pulse rectifier, and the THD of the input line current is maintained at 15.15%. When the turn ratio

$m$ of M-IPR is greater than 6.964, APDC will produce a pulse-doubling effect.

### B. Optimal Turn Ratio of M-IPR in APDC

When the turn ratio $m$ of M-IPR is greater than 6.964, the proposed rectifier operates under the three working modes mentioned above. From the analysis for the working modes, it is noticed that the output voltages of Rec1 and Rec2 are closely related to the turn ratio $m$ of M-IPR in APDC and the turn ratio $m$ directly affects the input current waveforms of the proposed rectifier. This section establishes the mathematical relationship between the turn ratio $m$ of M-IPR and the input line current to suppress the input current harmonics to the greatest extent.

As the three-phase input line currents are symmetrical, the phase "A" is taken as an example to calculate the optimal turn ratio to save space. In Fig. 1, from the KCL and MMF equation, the input line current $i_{\mathrm{A}}$ is obtained as

$$\begin{aligned} i_{\mathrm{A}}=&\tfrac{k}{\sqrt{3}}(S_{\mathrm{a1}}+\tfrac{\sqrt{3}-1}{2}S_{\mathrm{b1}}-\tfrac{\sqrt{3}+1}{2}S_{\mathrm{c1}})i_{\mathrm{d1}}\\ &+\tfrac{k}{\sqrt{3}}(\tfrac{\sqrt{3}+1}{2}S_{\mathrm{a2}}-\tfrac{\sqrt{3}-1}{2}S_{\mathrm{b2}}-S_{\mathrm{c2}})i_{\mathrm{d2}} \end{aligned} \tag{18}$$

where $S_{\mathrm{a1}}$ is the corresponding switching function between the currents $i_{\mathrm{a1}}$ and $i_{\mathrm{d1}}$, which satisfies

$$S_{\mathrm{a1}}=\begin{cases} 0 & \omega t\in[\frac{7\pi}{12},\frac{11\pi}{12})\cup[\frac{19\pi}{12},\frac{23\pi}{12})\\ 1 & \omega t\in[0,\frac{7\pi}{12})\cup[\frac{23\pi}{12},2\pi)\\ -1 & \omega t\in[\frac{11\pi}{12},\frac{19\pi}{12}). \end{cases} \tag{19}$$

According to the phase relation between switching functions, other switching functions can be obtained easily. In (18), it is clear that the input line current $i_{\mathrm{A}}$ is mainly determined by the output current $i_{\mathrm{d1}}$ and $i_{\mathrm{d2}}$ of Rec1 and Rec2. Combined with the working modes, the output current $i_{\mathrm{d1}}$ and $i_{\mathrm{d2}}$ of Rec1 and Rec2 can be obtained as

$$i_{\mathrm{d1}}=\begin{cases} \frac{1}{2}I_{\mathrm{d}} & \omega t\in[0,\theta]\\ \frac{2m}{2m+1}I_{\mathrm{d}} & \omega t\in[\theta,\frac{\pi}{6}-\theta]\\ \frac{1}{2}I_{\mathrm{d}} & \omega t\in[\frac{\pi}{6}-\theta,\frac{\pi}{6}+\theta]\\ 0 & \omega t\in[\frac{\pi}{6}+\theta,\frac{\pi}{3}-\theta]\\ \frac{1}{2}I_{\mathrm{d}} & \omega t\in[\frac{\pi}{3}-\theta,\frac{\pi}{3}] \end{cases} \tag{20}$$

$$i_{\mathrm{d2}}=\begin{cases} \frac{1}{2}I_{\mathrm{d}} & \omega t\in[0,\theta]\\ 0 & \omega t\in[\theta,\frac{\pi}{6}-\theta]\\ \frac{1}{2}I_{\mathrm{d}} & \omega t\in[\frac{\pi}{6}-\theta,\frac{\pi}{6}+\theta]\\ \frac{2m}{2m+1}I_{\mathrm{d}} & \omega t\in[\frac{\pi}{6}+\theta,\frac{\pi}{3}-\theta]\\ \frac{1}{2}I_{\mathrm{d}} & \omega t\in[\frac{\pi}{3}-\theta,\frac{\pi}{3}]. \end{cases} \tag{21}$$

In (20) and (21), $\theta$ is the phase angle and it is defined as the first phase angle when $|u_{\mathrm{m}}|=u_{\mathrm{d}}$ in the first period of $|u_{\mathrm{m}}|$. In terms of KVL and working modes of the proposed rectifier, the phase angle $\theta$ could be obtained as

$$\theta=\arctan\frac{1}{2m\left(2-\sqrt{3}\right)}. \tag{22}$$

Because the waveform of $i_{\mathrm{A}}$ is symmetrical, to save space, only the expression of $i_{\mathrm{A}}$ in the interval $\omega t\in[0,\pi/2]$ is given here. Substituting (19)–(21) into (18), the input line current $i_{\mathrm{A}}$ is obtained as

$$i_{\mathrm{A}}=\begin{cases} 0 & \omega t\in[0,\theta]\\ \frac{\sqrt{3}-1}{2}\frac{2m}{2m+1}kI_{\mathrm{d}} & \omega t\in[\theta,\frac{\pi}{6}-\theta]\\ \frac{\sqrt{3}+1}{4}kI_{\mathrm{d}} & \omega t\in[\frac{\pi}{6}-\theta,\frac{\pi}{6}+\theta]\\ \frac{2m}{2m+1}kI_{\mathrm{d}} & \omega t\in[\frac{\pi}{6}+\theta,\frac{\pi}{3}-\theta]\\ \frac{\sqrt{3}+3}{4}kI_{\mathrm{d}} & \omega t\in[\frac{\pi}{3}-\theta,\frac{\pi}{3}+\theta]\\ \frac{\sqrt{3}+1}{2}\frac{2m}{2m+1}kI_{\mathrm{d}} & \omega t\in[\frac{\pi}{3}+\theta,\frac{\pi}{2}-\theta]\\ \frac{\sqrt{3}+1}{2}kI_{\mathrm{d}} & \omega t\in[\frac{\pi}{2}-\theta,\frac{\pi}{2}]. \end{cases} \tag{23}$$

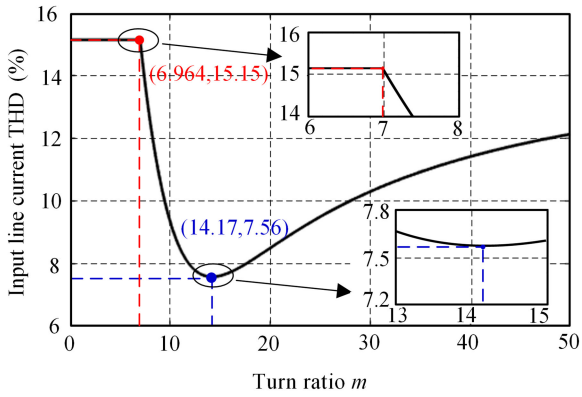


Fig. 6. Relationship between the input line current THD and turns ratio $m$.

In (23), the input line current $i_{\mathrm{A}}$ is mainly determined by the turn ratio $m$ of M-IPR in APDC.

In Fig. 1, if the turn ratio $m$ of M-IPR is less than 6.964, the maximum value of winding voltage $|u_{\mathrm{m}}|$ of M-IPR will not be greater than the minimum value of load voltage $u_{\mathrm{d}}$, and the auxiliary diodes $\mathrm{D_{m1}}$ and $\mathrm{D_{m2}}$ in APDC will be reverse-biased and turn OFF. In this case, the proposed rectifier works as a conventional 12-pulse rectifier, and the THD of the input line current is maintained at 15.15%. When the turn ratio $m$ of M-IPR is greater than 6.964, the auxiliary diodes $\mathrm{D_{m1}}$ and $\mathrm{D_{m2}}$ in APDC can be turned ON, and APDC will produce a pulse-doubling effect. At this time, the relationship between the input line current $i_{\mathrm{A}}$ and the turn ratio $m$ of M-IPR satisfies (23). According to the above analysis and (23), the relationship curve between the input line current THD and turn ratio $m$ of M-IPR is shown in Fig. 6.

As shown in Fig. 6, around the point (6.964, 15.15), if the turns ratio $m$ <6.964, then the auxiliary diodes $\mathrm{D_{m1}}$ and $\mathrm{D_{m2}}$ in the APDC are reverse-biased. The proposed rectifier works as a conventional 12-pulse rectifier and the THD of the input line current is maintained at 15.15%. For example, when $m=6$ or 6.5, the THD of the input line current are both 15.15%. If the turns ratio $m>$ 6.964, the auxiliary diodes $\mathrm{D_{m1}}$ and $\mathrm{D_{m2}}$ can turn ON, and the APDC generates a pulse-doubling effect. The input line current THD of the proposed rectifier decreases. For example, when the turns ratio $m=7.39$, the THD of the input line current decreases from 15.15% to 14%. Therefore, when

designing M-IPR, the turn ratio of M-IPR should be greater than 6.964.

With the increase of the M-IPR turn ratio $m$, the THD of the input line current first decreases and then increases. When the turns ratio $m = 14.17$, the THD of the input line current obtains the minimum value of 7.56%, which is the same as the input line current THD of a standard 24-pulse rectifier. In this certain case, the APDC helps double the 12-pulse rectifier into a standard 24-pulse rectifier. As depicted in Fig. 6, around the point (14.17, 7.56), the M-IPR turns ratio error has little effect on the input line current THD of the rectifier. For example, when the M-IPR turns ratio $m = 13$, the THD of the input line current is 7.66% and when the M-IPR turns ratio $m = 15$, the THD of the input line current is 7.6%, which indicates that around the optimal turn ratio ($m = 14.17$), about 10% of the turn ratio error of M-IPR only has not more than 0.1% impact on the THD of input line current. Therefore, the proposed scheme has good adaptability.

Under optimal turn ratio condition, the Fourier series expression of the input current $i_{\mathrm{A}}$ is

$$i_{\mathrm{A}} = kI_{\mathrm{d}} \sum_{n=1}^{\infty} B_{\mathrm{n}} \sin(n\omega t) \tag{24}$$

where

$$\begin{aligned} B_{\mathrm{n}} = &- \frac{8(\sqrt{3}+1)}{3n\pi} \sin^2 \frac{n\pi}{24} \cos\frac{n\pi}{8} \cos\frac{n\pi}{4} \cos n\pi \\ &\times \left(2\cos\frac{n\pi}{12} + 1\right) \\ &\left[\sqrt{2-\sqrt{3}}\cos\frac{5n\pi}{12} + \sqrt{2+\sqrt{3}}\cos\frac{n\pi}{12} + \sqrt{3}\cos\frac{n\pi}{6}\right. \\ &\left. + \sqrt{2}\cos\frac{n\pi}{4} + \cos\frac{n\pi}{3} + 1\right]. \end{aligned} \tag{25}$$

From (25), it can be seen that the input line current only contains $n = 24h \pm 1$ harmonic, and the input line current of the proposed rectifier presents the standard 24-pulse wave property.

### *C. Output Voltage of the Proposed Rectifier Under Optimal Turn Ratio Condition*

Under the optimal turn ratio condition, according to the working modes and the relationship between the output voltage $u_{\mathrm{d1}}$ and $u_{\mathrm{d2}}$ of Rec1 and Rec2 and the output voltage $u_{\mathrm{d}}$, the expression of $u_{\mathrm{d}}$ in one output voltage cycle $\omega t \in [0, \pi/12]$ can be obtained as

$$u_{\mathrm{d}} = \begin{cases} \frac{3}{4}(1+\sqrt{3})kU_{\mathrm{m}}\cos(\omega t) & \omega t \in [0, \frac{\pi}{24}] \\ \frac{3}{4}(1+\sqrt{3})kU_{\mathrm{m}}\cos(\omega t - \frac{\pi}{12}) & \omega t \in [\frac{\pi}{24}, \frac{\pi}{12}]. \end{cases} \tag{26}$$

In (26), the output voltage $u_{\mathrm{d}}$ has 24 pulses, and the output voltage ripple is reduced effectively. The average value of $u_{\mathrm{d}}$ is calculated as

$$U_{\mathrm{d}} = \frac{72\sqrt{2}km\cos\frac{11\pi}{24}}{(2m+1)\pi} U_{\mathrm{m}}|_{m=14.17} = 2.04kU_{\mathrm{m}}. \tag{27}$$

The above analysis showed that when the M-IPR in APDC takes the optimal turns ratio, the APDC extends the 12-pulse rectifier to the 24-pulse rectifier. The output voltage ripple is reduced effectively and the THD of the input current is reduced from 15.2% to 7.56%.

## IV. Capacity of the APDC

Under the optimal turn-ratio condition, the current $i_{\mathrm{m1}}$ flowing through the diode $\mathrm{D_{m1}}$ is obtained as follows in accordance with the working modes of ADPC:

$$i_{\mathrm{m1}} = \begin{cases} 0 & \omega t \in [0, \frac{5\pi}{24}] \\ 0.034I_{\mathrm{d}} & \omega t \in [\frac{5\pi}{24}, \frac{7\pi}{24}] \\ 0 & \omega t \in [\frac{7\pi}{24}, \frac{\pi}{3}]. \end{cases} \tag{28}$$

From (28), the maximum current through $\mathrm{D_{m1}}$ is only 3.4% $I_{\mathrm{d}}$. Compared with the double-tap changer scheme, the maximum current through the additional diodes is extensively decreased (from $I_{\mathrm{d}}$ to 3.4% $I_{\mathrm{d}}$). The additional conduction loss generated by the auxiliary $\mathrm{D_{m1}}$ could be calculated as

$$P_{\mathrm{Loss-D_{m1}}} = \int_0^{\pi/3} i_{\mathrm{m1}} d\omega t V_D = 0.0085 I_{\mathrm{d}} V_{\mathrm{D}} \tag{29}$$

where $\mathrm{V_D}$ is the forward voltage drop of auxiliary diodes $\mathrm{D_{m1}}$ and $\mathrm{D_{m2}}$.

As the APDC structure is symmetrical, the total additional conduction loss generated by the auxiliary diodes $\mathrm{D_{m1}}$ and $\mathrm{D_{m2}}$ is 0.017 $I_{\mathrm{d}}V_{\mathrm{D}}$. Compared with that of the double-tap changer scheme, the proposed scheme's additional conduction loss generated by the diodes is substantially decreased (from $I_{\mathrm{d}}V_{\mathrm{D}}$ to $0.017I_{\mathrm{d}}\mathrm{V_D}$) [18]–[20]. The proposed scheme has lower conduction losses and it is more preferable for large current applications than the double-tap changer scheme.

In accordance with (28), the root-mean-square (rms) values of the currents $i_{\mathrm{m1}}$ and $i_{\mathrm{m2}}$ could be obtained as

$$I_{\mathrm{m1\_rms}} = I_{\mathrm{m2\_rms}} = \sqrt{\frac{1}{2\pi}\int_0^{2\pi} i_{\mathrm{m1}}^2 d\omega t} = 0.017 I_{\mathrm{d}}. \tag{30}$$

The current $i_{\mathrm{AO}}$ flowing through the inner winding AO of APDC during one of its operating cycles could be calculated as

$$i_{\mathrm{AO}} = i_{\mathrm{m1}} + i_{\mathrm{d1}} = \begin{cases} 0.5I_{\mathrm{d}} & \omega t \in [0, \frac{\pi}{24}] \\ 0.034I_{\mathrm{d}} & \omega t \in [\frac{\pi}{24}, \frac{\pi}{8}] \\ 0.5I_{\mathrm{d}} & \omega t \in [\frac{\pi}{8}, \frac{5\pi}{24}] \\ 0.9659I_{\mathrm{d}} & \omega t \in [\frac{5\pi}{24}, \frac{7\pi}{24}] \\ 0.5I_{\mathrm{d}} & \omega t \in [\frac{7\pi}{24}, \frac{\pi}{3}]. \end{cases} \tag{31}$$

The rms value of the current $i_{\mathrm{AO}}$ is obtained as

$$I_{\mathrm{AO-rms}} = \sqrt{\frac{1}{2\pi}\int_0^{2\pi} i_{\mathrm{AO}}^2 d\omega t} = 0.5987 I_{\mathrm{d}}. \tag{32}$$

Considering that the APDC structure is symmetrical, the rms value of the inner winding BO of M-IPR in APDC are the same as that of the inner winding AO.

TABLE I
COMPARISON WITH THE SIMILAR RECTIFIER TOPOLOGIES

| Part | | Series-connected 24-pulse rectifier[21] | 24-pulse four-star rectifier[22] | 36-pulse AC–DC converter[23] | Proposed 24-pulse rectifier |
|---|---|---|---|---|---|
| Structure of the rectifier | | Series connection | Parallel connection | Parallel connection | Parallel connection |
| Input voltage of phase-shifting transformer | Shape | 24-step | sinusoidal | sinusoidal | sinusoidal |
| | Value | $U_{\mathrm{m}}$-$\omega LI_{\mathrm{m}}$ | $U_{\mathrm{m}}$ | $U_{\mathrm{m}}$ | $U_{\mathrm{m}}$ |
| Input current THD | | 2.65% | 5.25% | 3.1% | 3.9% |
| Displacement factor | | <1 | 1 | 1 | 1 |
| Number of input inductor | | 3 | 0 | 0 | 0 |
| Whether isolated | | isolated | isolated | non-isolated | isolated |
| Total magnectic ratings (% of output power) | | 131.93% | 162.99% | 30.51% | 123.06% |
| Strcuture of R-IPR/R-ST | | ST with the secondary center tapped windings | IPR with the added secondary center tapped windings | Double tapped IPR with the added secondary center tapped windings | Retrofitted double-tap IPR |
| Number of components | Transformer | 1 | 2 | 1 | 1 |
| | IPR | 0 | 2 | 0 | 0 |
| | R-IPR/R-ST | 1 | 1 | 1 | 1 |
| | Diode | 12 (main) 2 (auxiliary) | 12 (main) 2 (auxiliary) | 12 (main) 2 (auxiliary) 2 (high current stress) | 12 (main) 2 (auxiliary) |
| Conduction loss of additional auxiliary diodes | | Small | Small | Large | Small |
| Complexity | | Simple | Complicated | Slightly Complicated | Simple |
| Stability of the output voltage when the load changes | | Poor | Good | Good | Good |

Note: IPR, R-IPR, and R-ST are short for interphase reactor, retrofitted interphase reactor, and retrofitted single-phase transformer, respectively.

In Fig. 1, combining with the working cases, the input voltage $u_{\mathrm{p}}$ of APDC is obtained as

$$u_{\mathrm{p}}=\begin{cases}\frac{3}{2}(\sqrt{3}-1)kU_{\mathrm{m}}\sin(\omega t) & \omega t\in[0,\frac{\pi}{24}]\\ Y\cos(\omega t-\frac{\pi}{12}) & \omega t\in[\frac{\pi}{24},\frac{\pi}{8}]\\ \frac{3}{2}(1-\sqrt{3})kU_{\mathrm{m}}\sin(\omega t-\frac{\pi}{6}) & \omega t\in[\frac{\pi}{8},\frac{5\pi}{24}]\\ Y\cos(\omega t-\frac{\pi}{12}) & \omega t\in[\frac{5\pi}{24},\frac{7\pi}{24}]\\ \frac{3}{2}(\sqrt{3}-1)kU_{\mathrm{m}}\sin(\omega t-\frac{\pi}{3}) & \omega t\in[\frac{7\pi}{24},\frac{\pi}{3}]\end{cases} \tag{33}$$

where $Y=\frac{3\sqrt{2}(\sqrt{3}+\sqrt{2}-3)}{2(\sqrt{3}+\sqrt{2}-1)}kU_{\mathrm{m}}$.

The rms value of $u_{\mathrm{p}}$ is

$$U_{\mathrm{p\_rms}}=\sqrt{\frac{1}{2\pi}\int_0^{2\pi}u_{\mathrm{p}}^2d\omega t}=0.0575U_{\mathrm{d}}. \tag{34}$$

In accordance with the relationship between the M-IPR windings, the rms value of the voltages $u_{\mathrm{AM1}}$ and $u_{\mathrm{BM2}}$ of the windings AM1 and BM2 of M-IPR is obtained as

$$U_{\mathrm{AM1\_rms}}=U_{\mathrm{BM2\_rms}}=13.67U_{\mathrm{p\_rms}}=0.786U_{\mathrm{d}}. \tag{35}$$

Since the APDC structure is symmetrical, the equivalent capacity of APDC can be calculated as

$$\begin{aligned}S_{\mathrm{APDC}}&=\frac{U_{\mathrm{p\_rms}}}{2}I_{\mathrm{AO\_rms}}+U_{\mathrm{M1A\_rms}}I_{\mathrm{m1\_rms}}=0.0306U_{\mathrm{d}}I_{\mathrm{d}}\\&=3.06\%P_{\mathrm{d}}\end{aligned} \tag{36}$$

where $P_{\mathrm{d}}$ is the output power of the rectifier.

In (36), it is noticed that the capacity of APDC is only 3.06% of the output power so the proposed scheme has low cost and is simple to implement, and it can be used in high-power applications.

## V. COMPARISON WITH SIMILAR RECTIFIER TOPOLOGIES

To clarify the weaknesses and strengths of the proposed scheme, we initially compared the input line current THD, kVA ratings of magnetic elements, and number of components with the similar rectifiers [21]–[23] and the comparison results with similar rectifiers proposed in [21]–[23] are shown in Table I. Then, combined with the topological structure of the proposed rectifier and the similar rectifiers [21]–[23], the more comprehensive comparison results are given in this section.

### A. Comparison With the Series-Connected 24-Pulse Rectifier

Although the proposed rectifier and the series-connected 24-pulse rectifier [21] both suppress the input line current harmonics by adding an auxiliary circuit on the dc side of the rectifier, they have following significant differences.

1) The proposed rectifier is a parallel 24-pulse rectifier with an APDC at dc side. The APDC injects a specific square-wave current to modulate and increase the number of input current steps to 24 steps, and directly reduces the harmonic of the input line current. The rectifier in [21] is a series-connected 24-pulse rectifier with an auxiliary voltage injection circuit at dc side. The auxiliary voltage injection circuit injects a specific square-wave voltage to modulate and increase the number of input voltage steps to 24 steps, and then indirectly reduces the THD of the input current.
2) Although the input line current THD (2.1%) of the series-connected 24-pulse rectifier is slightly lower than that of the proposed rectifier (3.9%), the input side of the series-connected 24-pulse rectifier must be connected in series with three large enough inductors, otherwise the auxiliary voltage injection circuit on the dc side cannot

reduce the THD of the input line current. However, the large inductors in series on the input side not only reduce the DF of the rectifier but also lead to the softening of the output voltage characteristics of the rectifier. When the load current changes, the output voltage cannot be stabilized at a constant value. In addition, three large inductors in series on the dc side increase the volume and weight of the rectifier. Compared with the series-connected 24-pulse rectifier, the proposed rectifier does not need to connect large inductors in series on the ac side, which not only avoids the above problems caused by the series inductors on the ac side, but also reduces the volume and cost of the rectifier.

3) The total magnetic ratings (123.06% of output power) of the proposed rectifier are smaller than that (131.93% of output power) of the series-connected 24-pulse rectifier so the proposed rectifier has smaller size.

### *B. Comparison With the 24-Pulse Four-Star Rectifier*

The proposed 24-pulse rectifier and the 24-pulse 4-star rectifier [22] are equipped with APDCs on the dc side, and they have the same input and output characteristics as the standard 24-pulse rectifier. To further reduce the complexity of the pulse-doubling circuit in the 24-pulse 4-star rectifier, which is previously proposed in [22], the new APDC is proposed in this article. Compared with the 24-pulse 4-star rectifier, the proposed rectifier mainly has the following features.

1) Compared with the pulse-doubling circuit in the 24-pulse 4-star rectifier, the proposed APDC does not require addition of a secondary winding for the IPR. The modified IPR (M-IPR) has one less output terminal. The proposed APDC has simpler circuit structure and easier connection with the main circuit. In addition, its equivalent capacity is slightly reduced decreases from 3.1% of the output power to 3.06% of that.
2) The total magnetic rates (123.06% of output power) of the proposed rectifier is only 75.5% of the total magnetic rates (162.99% of output power) of the 24-pulse 4-star rectifier. The proposed rectifier has lower total magnetic rates and smaller size.
3) The 24-pulse 4-star rectifier requires 2 phase-shifting transformers, 2 conventional IPRs, and 1 IPR with center-tapped secondary winding. The proposed rectifier only requires one phase-shifting transformer and an improved tapped IPR. The proposed rectifier requires fewer magnetic components, and the circuit structure is simpler.

### *C. Comparison With the 36-Pulse AC–DC Converter*

Both the proposed rectifier and the 36-pulse ac–dc converter [23] suppress input current harmonics by introducing a pulse multiplication circuit on the dc side of the rectifier, but there are following differences between them.

1) Although the input line current THD (3.9%) of the proposed rectifier is slightly higher than that of the 36-pulse ac–dc converter (3.1%), the proposed APDC requires fewer components and has a simpler circuit structure with fewer lead-out terminals, and is easier to connect to the main circuit. The proposed APDC is composed of a modified IPR and two auxiliary diodes with low current stress. It is connected to the main circuit through five lead-out terminals. On the contrary, in the 36-pulse ac–dc converter, the pulse multiplication circuit is composed of a tapped IPR with a center-tapped secondary winding, two auxiliary diodes with low current stress, and two auxiliary diodes with high current stress. Moreover, seven lead-out terminals are connected to the main circuit.
2) Compared with the proposed rectifier, the pulse multiplication circuit in the 36-pulse ac–dc converter requires two low-current stress auxiliary diodes and two high-current stress auxiliary diodes. The two high-current stress diodes connected in series in the load path will produce higher additional conduction loss and reduce the efficiency of the rectifier.
3) The capacity of the tapped IPR with a center-tapped secondary winding in the 36-pulse ac–dc converter is 3.91% of the output power and that of the IPR in the proposed rectifier is 3.06% of the output power. The latter has a smaller equivalent capacity and volume.

## VI. Effects of Diode Open-Circuit Fault of APDC on the Harmonic Suppression Performance

Supposed that the diode $D_{m1}$ in APDC has an open-circuit fault and the diode $D_{m2}$ works normally. According to the working modes of APDC, there are only two working modes of APDC, namely O mode and P mode. According to the working mode of APDC, the output currents $i_{d1}$ and $i_{d2}$ of Rec1 and Rec2 is obtained as

$$i_{\mathrm{d1}} = \begin{cases} \frac{1}{2} I_{\mathrm{d}} & \omega t \in [0, \frac{5\pi}{24}] \\ \frac{2m}{2m+1} I_{\mathrm{d}} & \omega t \in [\frac{5\pi}{24}, \frac{7\pi}{24}] \\ \frac{1}{2} I_{\mathrm{d}} & \omega t \in [\frac{7\pi}{24}, \frac{\pi}{3}] \end{cases} \tag{37}$$

$$i_{\mathrm{d2}} = \begin{cases} \frac{1}{2} I_{\mathrm{d}} & \omega t \in [0, \frac{5\pi}{24}] \\ 0 & \omega t \in [\frac{5\pi}{24}, \frac{7\pi}{24}] \\ \frac{1}{2} I_{\mathrm{d}} & \omega t \in [\frac{7\pi}{24}, \frac{\pi}{3}]. \end{cases} \tag{38}$$

Substituting (37) and (38) into (18), the input current $i_{\mathrm{A}}$ of the proposed rectifier is obtained as

$$i_{\mathrm{A}} = \begin{cases} 0 & \omega t \in [0, \frac{\pi}{12}] \\ \frac{\sqrt{3}+1}{4} k I_{\mathrm{d}} & \omega t \in [\frac{\pi}{12}, \frac{5\pi}{24}] \\ \frac{2m}{2m+1} k I_{\mathrm{d}} & \omega t \in [\frac{5\pi}{24}, \frac{7\pi}{24}] \\ \frac{\sqrt{3}+3}{4} k I_{\mathrm{d}} & \omega t \in [\frac{7\pi}{24}, \frac{5\pi}{12}] \\ \frac{\sqrt{3}+1}{2} k I_{\mathrm{d}} & \omega t \in [\frac{5\pi}{12}, \frac{13\pi}{24}] \\ \frac{\sqrt{3}+1}{2} \frac{2m}{2m+1} k I_{\mathrm{d}} & \omega t \in [\frac{13\pi}{24}, \frac{5\pi}{8}] \\ \frac{\sqrt{3}+3}{4} k I_{\mathrm{d}} & \omega t \in [\frac{5\pi}{8}, \frac{3\pi}{4}] \\ \frac{\sqrt{3}+1}{4} k I_{\mathrm{d}} & \omega t \in [\frac{3\pi}{4}, \frac{7\pi}{8}] \\ \frac{\sqrt{3}-1}{2} \frac{2m}{2m+1} k I_{\mathrm{d}} & \omega t \in [\frac{7\pi}{8}, \frac{23\pi}{24}] \\ 0 & \omega t \in [\frac{23\pi}{24}, \pi]. \end{cases} \tag{39}$$

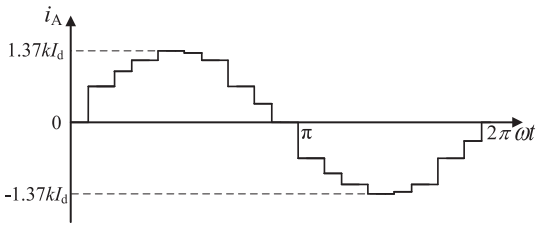


Fig. 7. Input line current $i_A$ when the diode $D_{m1}$ in APDC has an open-circuit fault.

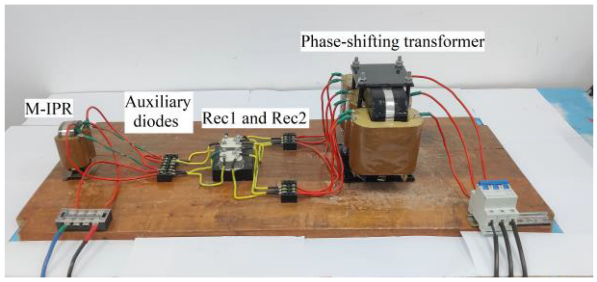


Fig. 8. Schematic diagram of the experimental prototype.

TABLE II
MAIN CIRCUIT PARAMETERS OF EXPERIMENTAL PROTOTYPE

| Parameter | Value |
|---|---|
| Input line-to-line voltage | 320V |
| Input voltage frequency | 50 Hz |
| Output current | 13A |
| Turn ratio $k$ of the zig-zag phase-shifting transformer | 0.25 |
| Load filter inductance | 15mH |
| Turn ratio $m$ M-IPR in APDC | 14.17 |
| Model of auxiliary diodes | FR207 |

According to (39), Fig. 7 shows the input line current $i_A$ when the diode $D_{m1}$ in APDC has an open-circuit fault.

As shown in Fig. 7, the input line current $i_A$ is a nonstandard 18-step wave. In this case, the THD of the input line current $i_A$ is 12%. Compared with those in a conventional 12-pulse rectifier, the step number of the input line current $i_A$ is increased from 12 to 18 and the input line current THD is decreased from 15.15% to 12%. This finding indicated that the proposed APDC still could reduce the input line current harmonics under the auxiliary diode open-circuit fault of APDC condition.

## VII. EXPERIMENTAL RESULTS

An experimental prototype with an output power of 1.7 kW was built to verify the pulse multiplier effect of APDC and the correctness of theoretical analysis. Fig. 8 shows the experimental prototype. The main circuit parameters of the experimental prototype are shown in Table II.

Under the parameters shown in Table II, the input line current $i_A$ and its spectrum of the rectifier with and without APDC are presented in Fig. 9(a) and (b), respectively.

When APDC is not used, the rectifier works as a conventional 12-pulse rectifier. As shown in Fig. 9(a), at this time, the input line current is a 12-step wave, and the input line current THD is

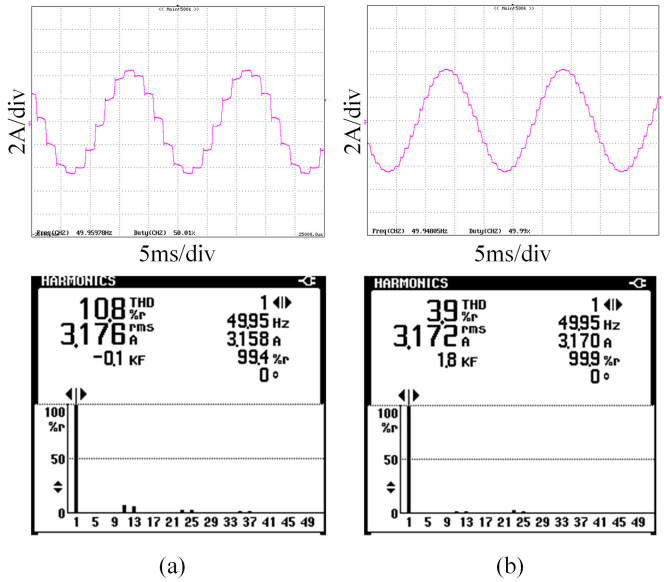


Fig. 9. Input line current and its spectrum. (a) Without APDC. (b) With APDC.

10.8%. After adopting APDC, as shown in Fig. 9(b), the number of steps of the input line current of the rectifier is doubled to 24. The input line current THD is effectively reduced from 10.8% to 3.9%. The main low-order harmonics, such as 11th and 13th, are decreased effectively from the input line current. Compared with the theoretical analysis result of (25), due to the slight asymmetry of the phase-shifting transformer structure, the 11th and the 13th input current harmonics have not been eliminated completely. Therefore, to obtain a better harmonic suppression effect, when manufacturing a phase-shifting transformer, it is necessary to improve its symmetry as much as possible. Due to the filtering effect of transformer leakage inductance, the THD of the input line current is slightly lower than the ideal value of 7.56%.

Fig. 10 shows the main current waveforms of the proposed 24-pulse rectifier with APDC on the dc side.

Fig. 10(a) shows the current $i_{m1}$ flowing through the auxiliary diode $D_{m1}$ in the APDC. The current $i_{m1}$ is a rectangular current with a frequency of 300 Hz and its amplitude is only 0.42 A, approximately 3.2% of the load current, basically consistent with the theoretical analysis results in Fig. 4(a). Fig. 10(b) shows that a rectangular current $i_s$ ($i_s = i_{m1}+i_{m2}$) is extracted by APDC from the dc side of the rectifier. This rectangular current has a frequency of 600 Hz and its amplitude is the same as that of $i_{m1}$. From the working modes of the proposed rectifier, it is noticed that the modulation of APDC increases the output current states of Rec1 and Rec2. As shown in Fig. 10(c), the output current of Rec1 is modulated to a three-level dc current, which is basically consistent with the analysis results shown in Fig. 4(c). Fig. 10(d) shows the input current of Rec1. Due to the modulation of APDC, the input current $i_{a1}$ is increased from three levels to five levels, whose shape and value are basically consistent with the theoretical analysis shown in Fig. 4(d).

Fig. 11(a) and (b) shows the output voltage waveforms of the rectifier without and with APDC, respectively.

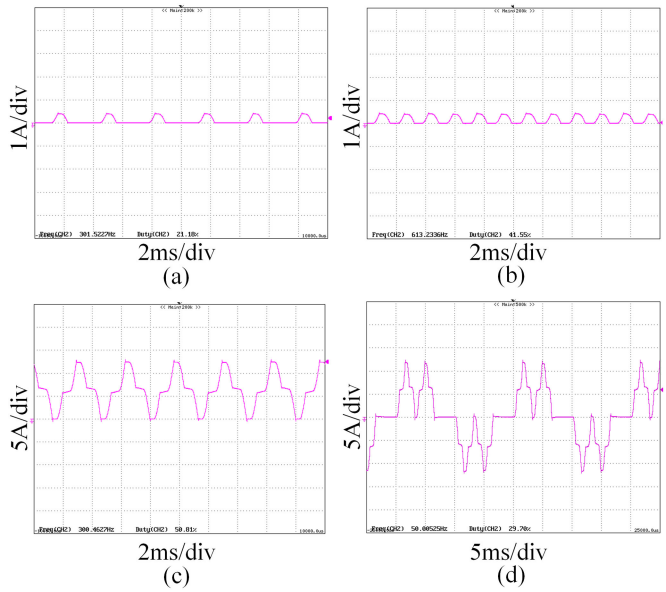


Fig. 10. Main waveforms of the proposed rectifier. (a) Current $i_{m1}$ flowing through $D_{m1}$. (b) Rectangular current $i_s$ ($i_s = i_{m1}+i_{m2}$) extracted by APDC from the dc side. (c) Output current $i_{d1}$ of Rec1. (d) Input current $i_{a1}$ of Rec1.

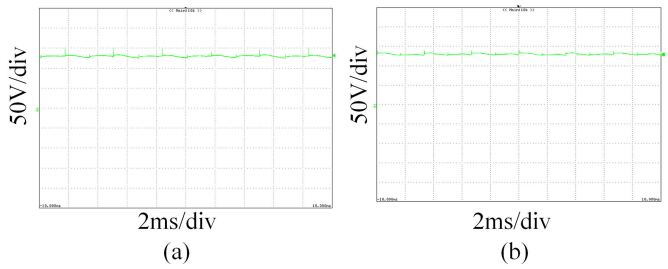


Fig. 11. Output voltage of rectifier. (a) Without APDC. (b) With APDC.

As shown in Fig. 11(a), when APDC is not adopted, the rectifier works as a conventional 12-pulse rectifier with an output voltage of 12 pulses, the average value of the output voltage is 130.2 V, the maximum value of the output voltage is 133.2 V, and the minimum value of the output voltage is 126.7 V. According to the definition of the output voltage ripple coefficient [24], the ripple coefficient of the output voltage in this certain case is 2.49%. As shown in Fig. 11(b), when the APDC is used, the pulse number of the output voltage is doubled to 24. However, the suppression effect of APDC on the output voltage ripple is not evident in Fig. 11 because the leakage inductance of the phase-shifting transformer increases the output voltage ripple and reduces the suppression effect of APDC on the output voltage ripple. In this case, the average output voltage of the rectifier is 130.7 V, the maximum output voltage is 133.7 V, the minimum output voltage is 128 V, and the ripple coefficient of the output voltage is 2.18%. This finding indicates that the output voltage ripple decreases slightly from 2.49% to 2.18% after using APDC.

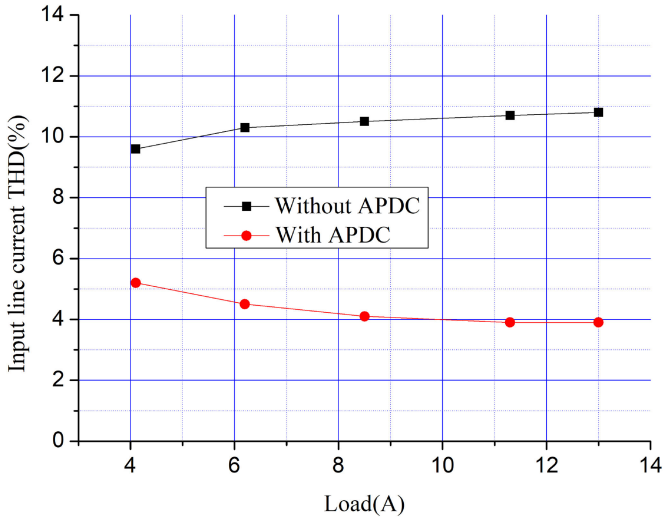


Fig. 12. Input line current THD under different load currents.

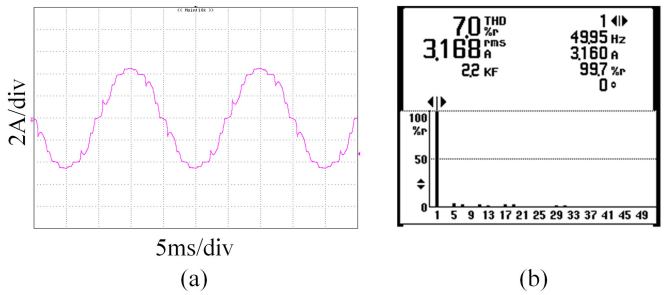


Fig. 13. Input line current $i_A$ and its spectrum when the auxiliary diode $D_{m1}$ in the APDC has an open-circuit fault. (a) Input line current $i_A$ (b) Spectrum of the input line current $i_A$.

Fig. 12 shows the THD of the input line currents when the load current varies from 4.1 to 13 A to validate the load adaptability of the proposed scheme.

Compared with those in conventional 12-pulse rectifiers, the input line harmonics are observably reduced due to the modulation of APDC. The input line current THD is less than 5% in a wide range of load current and it could meet the requirement of most industrial applications. The proposed rectifier provides a low-harmonic utility power interface.

When the auxiliary diode $D_{m1}$ in the APDC has an open-circuit fault, Fig. 13 shows the input line current $i_A$ and its spectrum.

As shown in Fig. 13, when the auxiliary diode $D_{m1}$ in the APDC has an open-circuit fault, the input current of the proposed rectifier becomes a nonstandard 18-step current, and the THD of the input line current is 7%, which is slightly less than the theoretical value 12% due to the filtering effect of transformer leakage inductance. By comparing with Fig. 9(a), it can be seen that the input line current THD is decreased from 10.8% to 7%. This indicates that when an open-circuit fault occurs in an auxiliary diode in the APDC, the proposed scheme still has a certain harmonic suppression effect.

## VIII. Conclusion

In this article, an APDC is proposed to extend the conventional 12-pulse rectifier to a new 24-pulse rectifier. Two low current stress auxiliary diodes are connected with the outer winding of the M-IPR in APDC, and they extract two rectangular currents from the dc side of the rectifier to shape the output current and voltage of three-phase rectification bridges first, which in turn double the pulse number of this rectifier. The resulting 24-pulse rectifier draws near-sinusoidal input line currents with less than 5% THD. The working modes of the proposed 24-pulse rectifier with APDC are analyzed and the optimal turns ratio of M-IPR in APDC is derived. When an auxiliary diode in APDC has an open-circuit fault, the harmonic suppression effect of APDC is also analyzed. The analysis results show that when an auxiliary diode in APDC has an open-circuit fault, APDC still has a certain harmonic suppression ability, which can reduce the THD of input current by more than 3%. Under the optimal turns ratio condition, the input line current THD reaches the smallest value and the maximum current through auxiliary diodes in APDC is only 3.4% of the output current. Compared with the double-tap changer scheme, the current stress and conduction loss of the additional diodes are effectively reduced. Since the capacity of APDC is only 3.06% of the output power, the proposed scheme has the advantages of simple circuit structure, low cost, and easy implementation.

## References


[1] B. Singh, S. Gairola, B. N. Singh, A. Chandra, and K. Al-Haddad, "Multipulse AC–DC converters for improving power quality: A review," *IEEE Trans. Power Electron.*, vol. 23, no. 1, pp. 260–281, Jan. 2008.

[2] J. Chen, Y. Shen, J. Chen, H. Bai, C. Gong, and F. Wang, "Evaluation on the autoconfigured multipulse AC/DC rectifiers and their application in more electric aircrafts," *IEEE Trans. Transp. Electrific.*, vol. 6, no. 4, pp. 1721–1739, Dec. 2020.

[3] J. S. Perisé, M. Bakkar, and S. B. Rodríguez, "Open-circuit fault diagnosis and maintenance in multi-pulse parallel and series TRU topologies," *IEEE Trans. Power Electron.*, vol. 35, no. 10, pp. 10906–10916, Oct. 2020.

[4] X. Li, W. Xu, and T. Ding, "Damped high passive filter—A new filtering scheme for multipulse rectifier systems," *IEEE Trans. Power Del.*, vol. 32, no. 1, pp. 117–124, Feb. 2017.

[5] M. S. Hamad, M. I. Masoud, K. H. Ahmed, and B. W. Williams, "A shunt active power filter for a medium-voltage 12-pulse current source converter using open loop control compensation," *IEEE Trans. Ind. Electron.*, vol. 61, no. 11, pp. 5840–5850, Nov. 2014.

[6] A. de Oliveira Costa Neto, A. L. Soares, G. B. de Lima, D. B. Rodrigues, E. A. A. Coelho, and L. C. G. Freitas, "Optimized 12-pulse rectifier with generalized delta connection autotransformer and isolated SEPIC converters for sinusoidal input line current imposition," *IEEE Trans. Power Electron.*, vol. 34, no. 4, pp. 3204–3213, Apr. 2019.

[7] P. Chen, X. Li, and Gong L, "A 12-pulse rectifier with an auxiliary circuit," *Proc. CSEE*, vol. 26, no. 23, pp. 163–166, Dec. 2006.

[8] M. M. Swamy, "An electronically isolated 12-pulse autotransformer rectification scheme to improve input power factor and lower harmonic distortion in variable-frequency drives," *IEEE Trans. Ind. Appl.*, vol. 51, no. 5, pp. 3986–3994, Sep./Oct. 2015.

[9] A. R. Izadinia and H. R. Karshenas, "Current shaping in a hybrid 12-pulse rectifier using a Vienna rectifier," *IEEE Trans. Power Electron.*, vol. 33, no. 2, pp. 1135–1142, Feb. 2018.

[10] M. Peterson and B. N. Singh, "A novel load compensator for a 12-pulse diode converter," in *Proc. IEEE Int. Conf. Power Electron. Drives Energy Syst.*, 2007, pp. 1–6.

[11] M. E. Villablanca, J. I. Nadal, and M. A. Bravo, "A 12-pulse AC–DC rectifier with high-quality input/output waveforms," *IEEE Trans. Power Electron.*, vol. 22, no. 5, pp. 1875–1881, Sep. 2007.

[12] S. Choi, P. N. Enjeti, H.-H. Lee, and I. J. Pitel, "A new active interphase reactor for 12-pulse rectifiers provides clean power utility interface," *IEEE Trans. Ind. Appl.*, vol. 32, no. 6, pp. 1304–1311, Nov./Dec. 1996.

[13] S. P. P. Kalpana, V. V. S., and B. Singh, "Investigations on open-circuit faults of zigzag autoconfigured transformer-based 12-pulse rectifier," *IEEE IEEE Trans. Ind. Appl.*, vol. 56, no. 2, pp. 1599–1608, Mar./Apr. 2020.

[14] V. Sheelvant, R. Kalpana, B. Singh, and P. P. Saravana, "Improvement in harmonic reduction of a zigzag autoconnected transformer based 12-pulse diode bridge rectifier by current injection at DC side," *IEEE Trans. Ind. Appl.*, vol. 53, no. 6, pp. 5634–5644, Nov./Dec. 2017.

[15] Y. Zhang, Z. Chen, B. Li, and Y. He, "Application of low harmonic 18-pulse rectifier power supply for radar power system," *IEEE Trans. Ind. Electron.*, vol. 66, no. 2, pp. 1080–1088, Feb. 2019.

[16] P. P. S., R. Kalpana, B. Singh, and G. Bhuvaneswari, "A 20-pulse asymmetric multiphase staggering autoconfigured transformer for power quality improvement," *IEEE Trans. Power Electron.*, vol. 33, no. 2, pp. 917–925, Feb. 2018.

[17] D. L. Mon-Nzongo, P. G. Ipoum-Ngome, T. Jin, and J. Song-Manguelle, "An improved topology for multipulse AC/DC converters within HVDC and VFD systems: Operation in degraded modes," *IEEE Trans. Ind. Electron.*, vol. 65, no. 5, pp. 3646–3656, May 2018.

[18] P. Qijun, M. Weiming, L. Dezhi, Z. Zhihua, and M. Jin, "A new critical formula and mathematical model of double-tap interphase reactor in a six-phase tap-changer diode rectifier," *IEEE Trans. Ind. Electron.*, vol. 54, no. 1, pp. 479–485, Feb. 2007.

[19] B. Singh, G. K. Kasal, and S. Gairola, "Power quality improvement in conventional electronic load controller for an isolated power generation," *IEEE Trans. Energy Convers.*, vol. 23, no. 3, pp. 764–773, Sep. 2008.

[20] R. Abdollahi and G. B. Gharehpetian, "Inclusive design and implementation of novel 40-pulse AC–DC converter for retrofit applications and harmonic mitigation," *IEEE Trans. Ind. Electron.*, vol. 63, no. 2, pp. 667–677, Feb. 2016.

[21] F. Meng, Q. Du, L. Wang, L. Gao, and Z. Man, "A series-connected 24-pulse rectifier using passive voltage harmonic injection method at DC-link," *IEEE Trans. Power Electron.*, vol. 34, no. 9, pp. 8503–8512, Sep. 2019.

[22] S. Yang, J. Wang, and W. Yang, "A novel 24-pulse diode rectifier with an auxiliary single-phase full-wave rectifier at DC side," *IEEE Trans. Power Electron.*, vol. 32, no. 3, pp. 1885–1893, Mar. 2017.

[23] P. Saravana Prakash, R. Kalpana, K. S. Chethana, and B. Singh, "A 36-pulse AC-DC converter with DC side tapped interphase bridge rectifier for power quality improvement," in *Proc. IEEE Int. Conf. Power Electron., Drives Energy Syst.*, 2018, pp. 1–5.

[24] F. Meng, L. Gao, S. Yang, and W. Yang, "Effect of phase-shift angle on a delta-connected autotransformer applied to a 12-pulse rectifier," *IEEE Trans. Ind. Electron.*, vol. 62, no. 8, pp. 4678–4690, Aug. 2015.


**Jingfang Wang** (Member, IEEE) was born in Hebei, China, in 1984. He received the B.S. degree in automation from Yanshan University, Qinhuangdao, China, in 2008, the M.S. degree in electrical engineering from Harbin Engineering University, Harbin, China, in 2012, and the Ph.D. degree in electrical engineering from the Harbin Institute of Technology, Harbin, China, in 2017.

He is currently a Lecturer of College of Intelligent Systems Science and Engineering, Harbin Engineering University. His research interests include high power converters and harmonics compensation.

**Anchen Chen** was born in Shandong, China, in 1993. He received the B.S. degree in physical geography and resource environment from the Shandong University of Science and Technology, Qingdao, China, in 2018, and the M.S. degree in electrical engineering from Harbin Engineering University, Harbin, China, in 2021.

He is currently an Assistant Engineer with CRRC Qingdao Sifang Rolling Stock Research Institute Co., Ltd., Qindao, China. His research interests include high power rectifiers and motor drives.

**Xuliang Yao** was born in Heilongjiang, China, in 1969. He received the B.S. degree in electrical engineering from the Harbin Institute of Technology, Harbin, China, in 1991, and the M.S. and Ph.D. degrees in control science and engineering from Harbin Engineering University, Harbin, China, in 2001 and 2006, respectively.

He had become a Lecturer with Harbin Engineering University during his Ph.D. study in 2002. He is currently a Professor with the College of Intelligent Systems Science and Engineering, Harbin Engineering University. He has authored or coauthored more than 40 papers. His research interests include high-power converters and motor driver technology.

**Lei Li** was born in Henan, China, in 1996. He received the B.S. degree in electrical engineering from the Harbin University of Science and Technology, Harbin, China, in 2019. He is currently working toward the M.S. degree in electrical engineering with Harbin Engineering University, Harbin, China.

His research interests include design and control of the multipulse rectifier.

**Yusheng Lv** was born in Henan, China, in 1997. He received the B.S. degree in automation from the North China University of Water Resources and Electric Power, Zhengzhou, China, in 2020. He is currently working toward the M.S. degree in electronic information with Harbin Engineering University, Harbin, China.

His research interests include harmonic suppression for high power rectifiers.

**Qiming Chen** (Member, IEEE) was born in Heilongjiang, China, in 1984. He received the B.E. degree from the Harbin University of Science and Technology, Harbin, China, in 2007, the M.E. degree from Harbin Engineering University, Harbin, China, in 2010, and the Ph.D. degree from the Harbin Institute of Technology (HIT), Harbin, China, in 2016.

Since 2020, he has been an Associate Research Fellow with the Laboratory for Space Environment and Physical Sciences, HIT, Harbin, China. His research interests include high power converters and motor drives.